A Novel Fault Detection and Fault Location Method for VSC-HVDC Links Based on Gap Frequency Spectrum Analysis

Yang, Q., Blond, S. L., Cornelusse, B., Vanderbemden, P. & Li, J.

DOI 10.1016/j.egypro.2017.12.625
ISSN 1876-6102
ESSN 1876-6102

Publisher: Elsevier

Available online at www.sciencedirect.com

ScienceDirect

Energy Procedia 142 (2017) 2243–2249

Energy Procedia

www.elsevier.com/locate/procedia

9th International Conference on Applied Energy, ICAE2017, 21-24 August 2017, Cardiff, UK

A Novel Fault Detection and Fault Location Method for VSC-HVDC Links Based on Gap Frequency Spectrum Analysis

Qingqing Yang[a], Simon Le Blond[b], Bertrand Cornelusse[c], Philippe Vanderbemden[c] and Jianwei Li[c]*

[a]*Beijing Electric Power Reseach Institute, Beijing Electric Power Company, State Grid, Beijing*
[b]*University of Bath, Bath, UK, BA2 6ER*
[c]*University of Liege, Liege 4000, Belgium*

Abstract

This paper proposes a one-end gap-based fault location method for VSC-HVDC transmission line using the fault current signal. Using the post-fault current time series, the frequency spectrum is generated for measuring the gaps between the contiguous peak frequencies. This method is able to locate the fault by analyzing the single-end fault current, which guarantees a faster response than using two-end data. The new gap-based approach is able to give accurate fault detection using any appropriate range of post-fault signal. Furthermore, the proposed method is fault resistance independent. A two-terminal VSC-HVDC system is modeled in PSCAD/EMTDC. The algorithm is verified by studying different cases of different fault resistances in various fault locations. The result shows that the proposed method gives an accurate and reliable fault location detection along DC transmission line. In addition, the proposed algorithm can be potentially used in other HVDC systems.

Peer-review under responsibility of the scientific committee of the 9th International Conference on Applied Energy.

Keywords: Fault current signal, fault detection,fault location transmission line, VSC-HVDC system.

1. Introduction

For HVDC transmission systems, during a fault, the DC line short circuit will not self-extinguished until the current reduces to zero [1]. Normally on HVDC point-to-point links, the circuit breakers reside on the AC side, and in the event of a fault, the entire link is de-energized. However, with increasing global requirements to transmit power on an inter-continental scale, and the development of new DC breakers, the benefits of a multi-terminal DC (MTDC) transmission system are becoming increasingly attractive [2, 3]. With MTDC, placing breakers on the AC side is not

* Corresponding author: Jianwei Li.
*E-mail address:*Jianwei.li@bath.edu

1876-6102
Peer-review under responsibility of the scientific committee of the 9th International Conference on Applied Energy .
10.1016/j.egypro.2017.12.625

acceptable since they will de-energise the whole system rather than isolating the faulted DC line. Therefore new methods are required for DC transmission line protection which is able to detect and isolate the faulted DC lines as fast as possible [4].

The HVDC system Fault location methods are an extremely important component to an effective design of a fault protection scheme [5]. A variety of fault location methods in HVDC systems are now in the prototype stage of development. Paper [4] has proposed an integrated traveling wave-based protection based on the zero and positive sequence backward traveling waves which can rapidly detect the fault type and faulty pole. The authors in [6] presents an algorithm that relies on the traveling wave principle using accurately detected surge arrival time at both terminals to determine the location of DC line faults. The wavelet transform is used to analyze travelling waves in [7] in an approach that deduces the fault direction from directional principles. Although travelling wave protection has the advantages such as fast operating speed and is robust to increased load and power swings [4, 6, 7], it also has some specific requirements for the network, such as high sampling rate and accurately identifying travelling wavefronts [8, 9]. In addition, travelling wave protection is vulnerable to lightening and other disturbances, as well as performing poorly on faults with high impedance [10]. Some other studies [3, 5, 8, 9] have described fault location methods based on system parameters. Compared with the travelling wave based methods, the approach based on system parameters has many advantages, such as high accuracy, independence of accuracy on the sampling frequency and the capability of giving the correct result from a number of signal window lengths and sizes, rather than relying on accurate detection just initial wave front [3, 8, 9]. Reference [8] uses the voltage signal measured at one terminal and matches its similarity to pre-existing recorded waveforms. The authors in [9] proposed a method to obtain the voltage distribution over the line from the measurement of voltage and current at both ends. Paper [3] proposes a method using high frequency components in the current signals detected at both ends of the line.

This paper uses a system parameters based method to develop a gap-based fault location detection algorithm using single-end fault current and analyzing the frequency component generated by these current signals. Some published work [11] have already shown that fault locations have a large impact on the frequency components of the current signals. The gap between the contiguous peak frequencies which has not been studied so far, but has a quantifiable relationship with the fault location. Therefore, this paper takes advantage of frequency analysis of the fault currents with different fault resistances at various fault locations and proposes a novel location algorithm. The validity of the new method is proved by cases studies. A dynamic point-to-point VSC-HVDC system is built in PSCAD/EMTDC, which is used to generate the fault signal. Finally, signal analysis and new algorithm implementation are achieved using MATLAB.

2. VSC-HVDC System Modeling

In this paper, a two-terminal VSC-HVDC system with a frequency dependent overhead line model is applied to demonstrate the novel method used in this paper. The VSC control method has already been used in many applications [12-14].The distributed parameter line model is used to produce very accurate fault frequency spectra. PSCAD/EMTDC is used to model a monopole transmission system (Fig. 1).

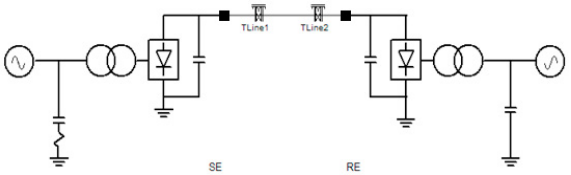

Fig. 1. Two-terminal VSC-HVDC system

Since a monopole system is considered in this work, only pole-to-ground fault can occur on the DC transmission line. Line-to-ground faults happen when a low impedance path occurs between the DC conductor and the ground, which is usually caused by lightning strikes or pollution. Under fault conditions, faults need to be detected quickly, and the faulted sections on both cables and overhead lines need to be blocked and tripped and thus isolated from the healthy system. Faults on cables are commonly permanent, but overhead lines can normally be restored after fault clearance, hence auto-reclosing is normally used on overhead lines [15]. Fast fault location is more important in

overhead lines than in cables since overhead line faults tend to be transient and thus auto reclosing restorative actions, based on zonal information are standard practice [16].

A pole-to-ground fault occurring at 2 s in the transmission line between two converter stations is simulated. By considering different situations based on different fault locations and different ground resistances, the analysis of transient components are derived. The granularity of variation is selected to cover the whole range of fault conditions. For varying locations, with fixed ground resistance, the ranges are set to be 10%, 30%, 50%, 70% and 90% on the transmission line at the rectifier side. The variation for resistance with the fault at particular fault location of the line is selected to be 0 Ω, 2 Ω, 10 Ω, 50 Ω and 100 Ω.

3. Fault Profile Analysis for Fault Location Scheme

Fault analysis on transmission lines is mainly based on the measurement of voltage and current with the features generated by the fault, which can generally be divided into time domain analysis and frequency domain analysis. This paper focuses on fault location on the DC side using current signals.

3.1. Current Signal Analysis

In response to the fault on transmission line with 0.01 Ω fault resistance with varying location, the time domain fault current waveform detected on the rectifier side is shown in Fig. 2 (a). The fault current waveform detected on faults occurring at 50% away from rectifier side with varying ground resistances are shown in Fig. 2 (b). The figures shown below are both from 1.8 s to 2.2 s selected from the whole simulation output. Faults are applied at 2 s as indicated.

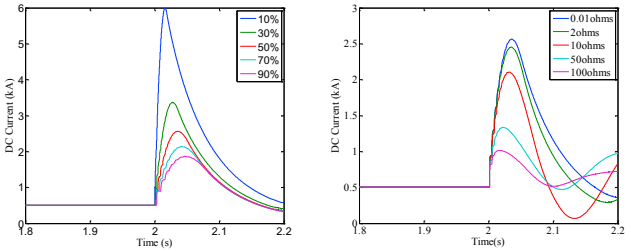

(a) 0.01ohms varying location (b) 50% with varying resistance

Fig. 2. Fault current detected from terminal 1

In response to the fault, the DC current through the rectifier end of the line will spike whatever the fault location and fault resistance is, while the current at the inverter side will drop. The short-circuit fault current will then return to the original current level after reaching the highest/lowest value. As can be seen in Fig. 2 (a), the fault current measured at the rectifier side is reduced while the distance between the fault point and the measuring point increases. The fault current also decreases as the fault resistance increases as shown in Fig. 2 (b).The fault current is attenuated due to the response of the converter station control system.

3.2. Current Signal Analysis

Fault current is generally affected by fault types, fault location on the transmission line, ground impedance, short-circuit capacity and other factors like converter stations. In addition, some faults are caused by the disconnection of a DC transmission line. During a fault, the transient signal contains many characteristic frequencies. The reason why high frequency component is considered to be the most significant factor in this paper is that the frequency components are more likely to be influenced by fault location rather than other factors like fault resistance. In an HVDC system, the transmission line protection zone is the area between two DC smoothing capacitors at the end of the line, which filter the characteristic harmonics from AC side. The frequency component is reduced by these DC smoothing capacitors. As a consequence, DC smoothing capacitors can be regarded as the boundary of the transmission of frequency components.

High impedance faults are generally challenging for many protection strategies because of the attenuation of the post-fault characteristics and thus its resemblance to steady state pre-fault conditions. However, in this paper, the fast Fourier transform (FFT) is used to obtain a frequency spectrum which contains a distinctive feature in the fault current

waveform, even in the case of high impedance faults. Analysis of these transient signals using the Fast Fourier Transform is an effective way to analyze the features generated by the fault.

The analysis of FFT is based on the data detected within 10ms beginning at the fault inception times of 2 s in the simulation. The specified frequencies can be easily obtained as shown in Fig. 3 (a)-(e) which indicate the fault location from 10% to 90% varying with fault resistance. Fig. 3 (f) shows the line varying with fault location under 0.01 Ω fault resistance.

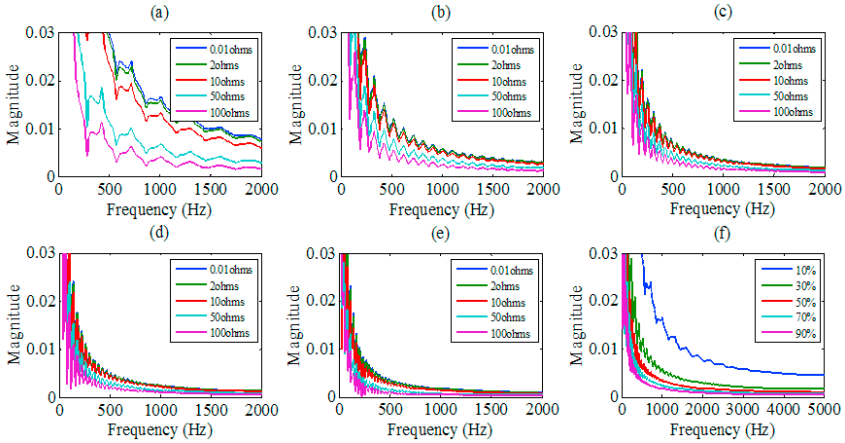

Fig. 3. Frequency spectrafor different fault locationsfrom the rectifier, varied from 10% (a) to 90% (e) and frequency spectra in 0.01 Ω fault resistance (f)

It can be seen that the shapes of frequency spectrum obtained from the current signal are similar for each specific fault location, regardless of fault resistance. The frequencies with peak values contain higher energy compared with other frequencies, where the frequencies with peak values are shown in Table 1. It means that the peaks appear in the fixed frequency band for a specific fault location, i.e. two contiguous peak frequencies have a specified gap with a fixed value during the fault occurring at a given location. The closer fault location is to the rectifier side, the larger the gap between two frequencies with peak values. The frequencies spike at a group of specified frequencies no matter where the fault location is. Regardless of the magnitude difference caused by fault resistance, the features between fault location and frequencies are apparent.

Table 1. Frequency Spectrum Peak Value Analysis

Fault Location	Frequency Peak Value (Hz)
10% from T1	140,430,720,1010,1300,1590,1880, etc.
30% from T1	140,240,330,430,520,620,720,810,910,1010,1100,1200,1300,1400,1490,1590,1690,1790,1880,etc.
50% from T1	80,140,200,250,310,370,430,480,540,600,660,720,770,830,890,950,1010,1070,1120,1180,1240,1300,1360,1420,1480,1530,1590,1650,1710,1770,1830,1880,etc.
70% from T1	60,100,140,180,220,260,300,340,390,430,470,510,550,590,630,690,720,760,800,840,880,920,970,1010,1050,1090,1130,1170,1220,1260,1300,1340,1380,1420,1470,1510,1550,1590,1630,1680,1760,1800,1840,1880,etc.
90% from T1	50,80,100,140,170,200,240,270,300,330,360,390,430,460,490,520,560,590,620,650,680,720,750,780,810,850,880,910,940,980,1010,1040,1070,1110,1140,1170,1200,1240,1270,1300,1330,1370,1400,1430,1460,1500,1530,1590,1630,1660,1690,1720,1760,1790,1820,1850,1880,etc.

The current signal used in analysis is 10 ms long, beginning at 2 s. However, it can also be seen that similar frequency spectra are generated with different section of post-fault signal with the same range of duration of 10 ms signal starting from 2.01 s. Hence, for this method any appropriate range of post-fault signal in any sections of the signal can be used for detection. In conclusion, despite the magnitude variations caused by different fault resistance, the overall shape of the frequency spectra generated by current signal is similar for a specific fault location. This feature can be used as the basis of a fault location method.

3.3. Current Signal Analysis

The proposed technique is based on the estimation of transmission line fault current transient signal at the capacitor point of connection on DC side. By applying the FFT to these detected current signals, the frequency spectrum is generated to analyze the relationship between frequencies and fault location. The basic design of the protection scheme is shown as a flowchart in Fig. 4. Numerous peak components are generated in the whole frequency band, and the frequencies with peak magnitudes are expected to be detected corresponding to a specified range of frequencies, as can be seen in Fig. 5, between f_n and f_{n-1}.

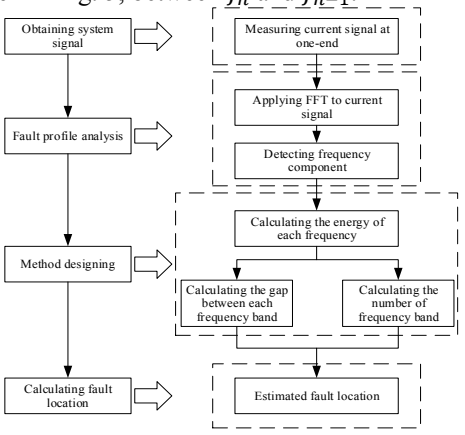

Fig. 4. Flowchart of method design

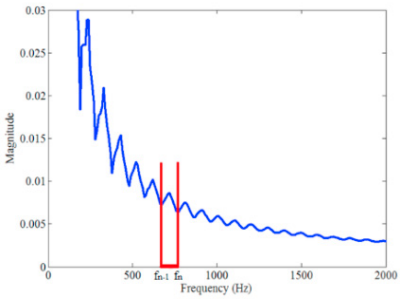

Fig. 5. Example of a magnitude spectrum

At different fault locations, the fault currents have their specified peak and valley value in a frequency band. If with fixed gap between two contiguous peak frequencies, the frequency with peak value can be expressed in (1):

$$f_p = f_o + (2N+1)\Delta f \tag{1}$$

Where: N is an integer starting from 0, f_o is the original frequency, f_p is the frequency with peak value in a frequency band, and $\Delta f_n = f_n - f_{n-1}$ is the gap between two adjacent frequencies.

However, the gaps between two contiguous frequencies are not always the same. Based on the FFT frequency measurement introduced in [17], the frequency spectrum has a peak magnitude at f_n in range of Δf. The energy for each peak frequency band can be computed as (2):

$$\Gamma(f_n) = \sum_{j=1}^{N} \left[i_{f_n}^{p}(j) \right]^2 \tag{2}$$

Based on the peak frequency detection, the average gap between frequencies can be calculated (3).

$$G_{Ave} = \frac{\sum_{n=1}\{arg|_{f_n} max[\Gamma(f_n)] - arg|_{f_{n-1}} max[\Gamma(f_{n-1})]\}}{C_G}, \qquad \left(f_n < \frac{f_s}{2}\right) \tag{3}$$

Where: C_G is the total number of frequency bands detected, f_s is the sampling frequency. Hence, equation (4) was developed to estimate the fault distance D, in percentage line length from breaker on the rectifier side.

$$D = \varepsilon G_{Ave} \tag{4}$$

Where: D is the fault location, ε is a coefficient determined empirically by careful study of the spectra for the specific system, G_{Ave} is the average value of gap between frequency bands.

3.4. Current Signal Analysis

In order to verify the validity of the proposed method, pole-to-ground faults were simulated at different locations with different fault resistances. According to the proposed method expressed in flowchart shown in Fig.4, the fault location result is calculated, which is shown in Table 2.The accuracy of the method has been evaluated with (5) to calculate the relative error:

$$e = \left| \frac{D_{act} - D_{det}}{L} \right| \tag{5}$$

Where: D_{act} is actual fault location from the measuring terminal, D_{det} is the detected fault location and L is the total length of the transmission line.

The results show that the proposed method can accurately locate faults with the largest relative error, calculated by (5), being less than 1% no matter what fault resistance is, which is in a fairly acceptable range. It is worth noting that the overall average error for pole-to-ground faults is 0.313% which means that the fault location algorithm is very accurate. As can be seen from Table 2, the further the fault location to the measuring end, the larger the error is in the fault location scheme. Hence, a further study with the detection of two-end data can be made to increase the accuracy of fault location. Even though two-end data estimation requires greater response time of the system and the telecommunication between two converters, a more robust fault location method can be obtained with two-end data.

Table 2. Fault Location Result

Fault Location	**Measured Distance**					**Average Error**
	0.01 Ω	2 Ω	10 Ω	50 Ω	100 Ω	
12%	12.32%	11.72%	12.30%	12.45%	11.87%	0.296%
36%	36.16%	35.52%	36.36%	35.62%	36.47%	0.237%
47%	47.12%	46.67%	47.37%	46.85%	47.62%	0.318%
76%	75.72%	75.39%	76.45%	76.43%	75.67%	0.42%
84%	83.74%	84.05%	83.49%	83.93%	84.58%	0.294%

4. Conclusion

In this paper, a two-terminal VSC-based HVDC model is implemented in PSCAD/EMTDC with a pole-to-ground fault simulated in the DC transmission system. Fault signals are generated with this model, giving insights into the characteristic frequency components contained within the signal. A detailed fault current profile is analyzed, and the frequency spectrum is generated using MATLAB. Through the relationship between the difference in two contiguous peak frequencies and the distance of fault location, a novel fault location method is proposed based on the gap of two contiguous peak frequencies. The most important achievement presented in this proposed fault location method for VSC-HVDC transmission lines is that only measurements from a single terminal are used to increase response time. In addition, any sections of post-fault signal can be used unlike the traveling-wave methods that use only the initial wavefront to locate fault. Finally the method is robust to high resistance faults. In addition to these features, the algorithm is shown to have high reliability and high accuracy.

References

[1] Li J, Zhang M, Zhu J, Yang Q, Zhang Z, Yuan W. Analysis of Superconducting Magnetic Energy Storage Used in a Submarine HVAC Cable Based Offshore Wind System. Energy Procedia. 2015;75:691-6.

[2] Yang Q, Le Blond S, Liang F, Yuan W, Zhang M, Li J. Design and application of superconducting fault current limiter in a multiterminal HVDC system. IEEE Transactions on Applied Superconductivity. 2017;27:1-5.

[3] Yang Q, Le Blond S, Aggarwal R, Wang Y, Li J. New ANN method for multi-terminal HVDC protection relaying. Electric Power Systems Research.2017; 148;192-201

[4] Ying Z, Nengling T, Bin X. Fault Analysis and Traveling-Wave Protection Scheme for Bipolar HVDC Lines. Power Delivery, IEEE Transactions on. 2012;27:1583-91.

[5] Jin Y, Fletcher JE, O'Reilly J. Short-Circuit and Ground Fault Analyses and Location in VSC-Based DC Network Cables. Industrial Electronics, IEEE Transactions on. 2012;59:3827-37.

[6] Nanayakkara OMKK, Rajapakse AD, Wachal R. Location of DC Line Faults in Conventional HVDC Systems With Segments of Cables and Overhead Lines Using Terminal Measurements. Power Delivery, IEEE Transactions on. 2012;27:279-88.

[7] Aguilera C, Orduna E, Rattá G. Directional traveling-wave protection based on slope change analysis. Power Delivery, IEEE Transactions on. 2007;22:2025-33.

[8] Farshad M, Sadeh J. A Novel Fault-Location Method for HVDC Transmission Lines Based on Similarity Measure of Voltage Signals. Power Delivery, IEEE Transactions on. 2013;28:2483-90.

[9] Jiale S, Shuping G, Guobing S, Zaibin J, Xiaoning K. A Novel Fault-Location Method for HVDC Transmission Lines. Power Delivery, IEEE Transactions on. 2010;25:1203-9.

[10] Zou G, Gao H, Su W, Wang D. Identification of lightning stroke and fault in the travelling wave protection. Journal of Electromagnetic Analysis and Applications. 2009;2009.

[11] Yang Q, Le Blond S, Aggarwal R, Wang Y, Li J. New ANN method for multi-terminal HVDC protection relaying. Electric Power Systems

Research. 2017;148:192-201.

[12]. Li J, Gee AM, Zhang M, Yuan W. Analysis of battery lifetime extension in a SMES-battery hybrid energy storage system using a novel battery lifetime model. Energy. 2015;86:175-85.

[13]. Li J, Wang X, Zhang Z, Le Blond S, Yang Q, Zhang M, et al. Analysis of a new design of the hybrid energy storage system used in the residential m-CHP systems. Applied Energy. 2017;187:169-79

[14]. Li J, Yang Q, Robinson F, Liang F, Zhang M, Yuan W. Design and test of a new droop control algorithm for a SMES/battery hybrid energy storage system. Energy. 2017;118:1110-22.

[15] Jie Y, Jianchao Z, Guangfu T, Zhiyuan H. Characteristics and Recovery Performance of VSC-HVDC DC Transmission Line Fault. Power and Energy Engineering Conference (APPEEC), 2010 Asia-Pacific2010. p. 1-4.

[16] Jiebei Z, Booth C. Future multi-terminal HVDC transmission systems using Voltage source converters. Universities Power Engineering Conference (UPEC), 2010 45th International2010. p. 1-6.

[17] Li J, Xiong R, Yang Q, Liang F, Zhang M, Yuan W. Design/test of a hybrid energy storage system for primary frequency control using a dynamic droop method in an isolated microgrid power system. Applied Energy. 2017;201:257-69.